

# Bandwidth and Fermi surface of Iron-Oxypnictides: covalency and sensitivity to structural changes

Veronica Vildosola,<sup>1,2,3</sup> Leonid Pourovskii,<sup>1</sup> Ryotaro Arita,<sup>4,3</sup> Silke Biermann,<sup>1,3</sup> and Antoine Georges<sup>1,3</sup>

<sup>1</sup>*Centre de Physique Théorique, École Polytechnique, CNRS, 91128 Palaiseau, France*

<sup>2</sup>*Departamento de Física, Comisión Nacional de Energía Atómica (CNEA-CONICET),  
Provincia de Buenos Aires, San Martín, Argentina*

<sup>3</sup>*Japan Science and Technology Agency, CREST*

<sup>4</sup>*Department of Applied Physics, University of Tokyo, Tokyo 113-8656, Japan*

Some important aspects of the electronic structure of the iron oxypnictides depend very sensitively on small changes in interatomic distances and bond angles within the iron-pnictogen subunit. Using first-principles full-potential electronic structure calculations, we investigate this sensitive dependence, contrasting in particular LaOFeAs and LaOFeP. The width of the Fe-bands is significantly larger for LaOFeP, indicating a better metal and weaker electronic correlations. When calculated at their experimental crystal structure these two materials have significantly different low-energy band structure. The topology of the Fermi surface changes when going from LaOFeP to LaOFeAs, with a three-dimensional hole pocket present in the former case transforming into a tube with two-dimensional dispersion. We show that the low-energy band structure of LaOFeAs evolves towards that of LaOFeP as the As atom is lowered closer to the Fe plane with respect to its experimental position. The physical origin of this sensitivity to the iron-pnictogen distance is the covalency of the iron-pnictogen bond, leading to strong hybridization effects. To illustrate this, we construct Wannier functions, which are found to have a large spatial extension when the energy window is restricted to the bands with dominant iron character. Finally, we show that the Fe bandwidth slightly increases as one moves along the rare-earth series in ReOFeAs and discuss the physical origin of this effect.

PACS numbers:

## Introduction

The recent discovery of superconductivity in electron-doped rare-earth oxyarsenides<sup>1</sup> has generated a great deal of interest in the electronic structure and magnetic properties of these compounds, with different types of magnetic<sup>2,3</sup> or charge<sup>4</sup> fluctuations conjectured to be at the origin of the pairing mechanism.

The rare-earth iron oxyarsenides belong to a wider class of rare-earth oxypnictides  $ReOTPn$  (where  $Re$  and  $T$  are the rare-earth and transition metals, respectively,  $Pn = P, As$  is the pnictogen ion, with nominal charge  $-3$ ) which have the same tetragonal structure of ZrCuSiAs-type<sup>6</sup>. In spite of obvious similarities in the overall electronic structure, those compounds differ in their magnetic properties and their tendency towards superconductivity. It is particularly interesting in this respect to contrast the properties of LaOFeAs to those of its phosphate homologue LaFeOP. Relating the observed differences to relevant differences in their electronic structure may provide important clues into the nature and the origin of magnetism and superconductivity in these materials. The undoped stoichiometric compounds have different magnetic properties: LaOFeP is non-magnetic<sup>8</sup>, while LaOFeAs undergoes a magnetic ordering transition at a temperature of 134 K<sup>1</sup> preceded by a structural transition at a slightly higher temperature<sup>5</sup>. Their transport properties above the magnetic transition temperatures are also different, with the electrical conductivity of LaOFeP being substantially larger than that of LaOFeAs<sup>1,9</sup>. These compounds also differ signifi-

cantly in their superconducting properties. While undoped LaOFeAs is magnetic and non-superconducting, the situation in the absence of doping for the parent compound LaOFeP is currently somewhat controversial. A superconducting transition in the range 4-7 K was originally reported<sup>7</sup>, and recently confirmed in Ref. 9, but questioned in Ref. 10 which found no superconductivity above 0.35 K. At any rate, electron doping suppresses the antiferromagnetism in LaOFeAs and leads to a superconducting phase with  $T_c$  as high as 26 K, while it does not induce such drastic changes in the phosphate compound, in which it causes only a moderate increase of  $T_c$  up to 8 K<sup>9</sup>.

The electronic structure of the LaOFeP compound, in particular its Fermi surface (FS), has been investigated theoretically by Lebegue<sup>11</sup>. His results can be outlined as follows: the LaOFeP FS consists of two ellipsoidal electronic cylinders centered at the  $M - A$  line at the Brillouin zone (BZ) edge, and of two hole cylinders centered at the BZ center  $\Gamma - Z$  line, together with a single hole pocket with three-dimensional (3D)-like dispersion at the  $Z$  point. A basically identical shape of the FS has been proposed in several theoretical papers<sup>12,13,14</sup> for LaOFeAs, with electron doping resulting in the disappearance of the 3D-hole pocket, which gets filled, thus changing the FS topology and increasing the two-dimensional character upon doping. This topological change and reduction of effective dimensionality has been suggested to be at the origin of the different types of magnetic fluctuations observed in the stoichiometric and doped LaOFeAs compounds, respectively<sup>3,14</sup>,

and possibly also responsible for the appearance of superconductivity in the doped compound. It is important to note, in this respect, that most electronic structure calculations in Refs.<sup>12,13,14</sup> have been carried out at values of the lattice constants and internal parameters (the Fe-As and La-O interplane distances) which were obtained by relaxing the structure within LDA/GGA. As pointed out very recently by Mazin *et al.*<sup>14</sup>, rather small changes in the LaOFeAs structural parameters, particularly, in the Fe-As interatomic distance, may lead to the disappearance of the 3D hole pocket from the FS of stoichiometric LaOFeAs. Furthermore, internal parameters of the LaOFeAs experimental crystal structure are rather poorly reproduced by theoretical LDA/GGA calculations, with the Fe-As interplane distance being underestimated by about 6%<sup>15</sup>.

For these reasons, a comparative study of the LaOFeP and LaOFeAs compounds is especially relevant in order to clarify the relations between electronic properties and the electronic structure of these materials. We *do know* that stoichiometric LaOFeP and LaOFeAs differ substantially, particularly in properties directly related to the low-energy electronic structure such as magnetic ordering, transport or superconductivity. Therefore, one may hope and expect that electronic structure calculations carried out at judiciously chosen structural parameters should be able to capture this difference. In this article, we carry out a detailed first-principles investigation of LaOFeAs and LaOFeP aimed at identifying relevant differences in their electronic structures while relating them to the small but significant differences which exist between the LaOFeAs and LaOFeP lattice structures. We show that electronic structure calculations at the *experimental* lattice parameters and internal positions result in the Fermi surfaces of LaOFeP and LaOFeAs having different shapes, with the 3D hole pocket present in the case of LaOFeP, but not in the case of LaOFeAs. These changes in the FS topology are due to shortening of the iron-pnictogen bond-length in LaOFeP as compared to LaOFeAs. We identify the sensitivity of the electronic structure to this bond-length as being due to the rather high degree of covalency associated with the iron-pnictogen bond, and illustrate this point by constructing appropriate Wannier functions.

The paper is organized as follows. We briefly outline our calculational approach in Sec. I. The overall electronic structure of LaOFeAs and LaOFeP is discussed in Sec. II. Low-energy aspects of this electronic structure and Fermi surfaces are described in Sec. III, and the differences between the two materials are illustrated by a study of the sensitivity of these low-energy aspects to the Fe-pnictogen distance. Then, in Sec. IV, we perform a Wannier function construction which illustrates this sensitivity and relates it to the covalency of the iron-pnictogen bond. Finally, in Sec. V we study the influence of the structural properties on the width of the Fe- bands and its material dependence.

Table I: Crystal-structure data for LaOFeAs<sup>5</sup> and LaOFeP<sup>7</sup>. Lattice constants  $a$  and  $c$ , internal positions of the  $Pn$  and La ( $z$ ) in units of  $c$ , and the vertical distance of the  $Pn$  with respect to the Fe plane ( $d_v$ ). The vertical distance is related to the  $z$ -parameter by  $d_v = (z - 0.5)c$ , and the angle  $\theta$  between the As-Fe bond and the Fe-plane by  $\tan(\theta) = (2z - 1)c/a$ .

	LaOFeAs	LaOFeP
$a$	4.0301 Å	3.9636 Å
$c$	8.7368 Å	8.5122 Å
$z(\text{La})$	0.1418	0.1487
$z(Pn)$	0.6507	0.6339
$d_v$	1.32 Å	1.14 Å
$\theta$	33.2°	29.9°
$d_{Fe-As}$	2.41 Å	2.33 Å

## I. COMPUTATIONAL DETAILS

The first principle calculations of the band-structure and Fermi surface of these materials presented in Sec. II and Sec. III were performed using the Full-Potential APW+local orbitals method as implemented in the Wien2k<sup>16</sup> code. We considered 800  $\mathbf{k}$ -points in the BZ and checked that all the properties presented in this article were converged with this mesh. The results that we present here have been obtained within the Local Density Approximation (LDA)<sup>17</sup> to the exchange-correlation potential but it is worth mentioning that our conclusions do not vary if we use the generalized-gradient approximation (GGA)<sup>18</sup> instead. We have also performed a calculation using the Quantum-ESPRESSO package<sup>19</sup>, with the computational details like in 20, and constructed maximally localized Wannier functions<sup>21</sup> by using the code developed by Mostofi *et al.*<sup>22</sup>. Last but not least, we have performed an Nth order muffin tin orbital construction for the Fe-d orbitals<sup>23</sup>.

## II. BAND STRUCTURE OF LaOFeAs AND LaOFeP : COMPARISON ON A LARGE ENERGY-SCALE

In this section, we compare the calculated band structure of LaOFeP and LaOFeAs at their experimental crystal structure, on a large energy scale covering the whole Fe,  $Pn$  (=As or P) and O bands as shown in Fig. 1. The crystal structure parameters were taken from experiments and are given in Table I.

The obtained bandstructures for both materials are depicted on Fig. 1. In this figure, the colors of the bands are simply guides to the eyes in order to compare more easily their relative positions and bandwidths. The bands plotted in red and green have mainly Fe  $3d$  and  $Pn$ -O  $p$  character, respectively. The bands shown in black correspond mainly to La  $4f$  states which are well above the Fe bands. The blue arrows in between the two plots show

the approximate bandwidth of the Fe  $3d$  bands in each compound. One may observe that the bands that are close to the Fermi level, which correspond to Fe, have larger bandwidth in LaOFeP as compared to LaOFeAs. This is a plausible explanation of why the former is observed to be a better metal (in the sense of smaller resistivity)<sup>1,7</sup>. This also indicates a lesser degree of electronic correlations in LaOFeP.

The difference in bandwidth results from a combination of three factors. First, from the difference in Fe-Fe distance which is significantly smaller in LaOFeP. Secondly, P and As have different electronegativity, which leads to a shift towards more negative energies of the P-bands in LaOFeP. Finally, the  $Pn$  has different vertical distances with respect to the Fe plane, a quantity which is mainly governed by the internal  $z$  parameter, and may influence the width of the Fe's bands through the different strength of the Fe- $Pn$  bond.

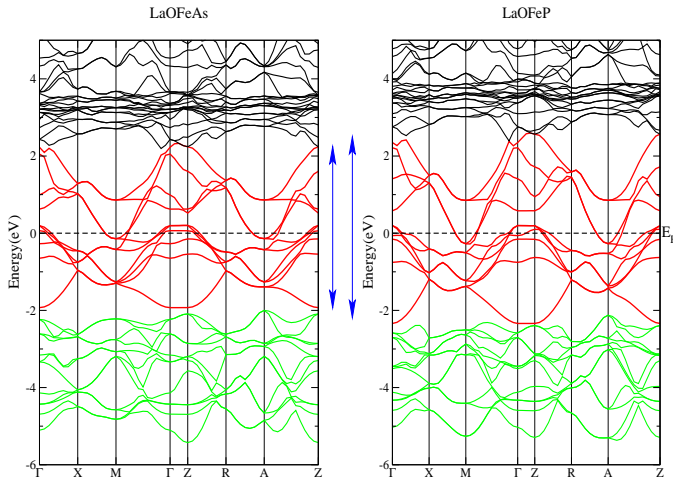


Figure 1: Band structure of LaOFeAs (left) and LaOFeP (right). Red and green bands have mainly Fe-3d and Pnictogen/Oxygen-p character respectively. The colors are guides to the eyes in order to facilitate comparison of the relative positions and widths of the bands ( see also blue arrows).

### III. LOW-ENERGY BANDSTRUCTURE AND FERMI SURFACE: GREAT SENSITIVITY TO FE-PN DISTANCE

In this section, we focus on the very low-energy band structure and Fermi surface properties of the LaOFeAs and LaOFeP compounds, as depicted on Fig. 2 and Fig. 3 (calculated for the experimental crystal structure as given in Table I).

In both compounds, the Fermi level is crossed by five bands with mainly Fe character. Both materials present two electron pockets centered at M and two hole pockets centered at  $\Gamma$  with mainly  $d_{xz}$  and  $d_{xz/yz}$  character. (Our choice of the local coordinate system centered at Fe is such that the  $x/y$  axes point towards the nearest-

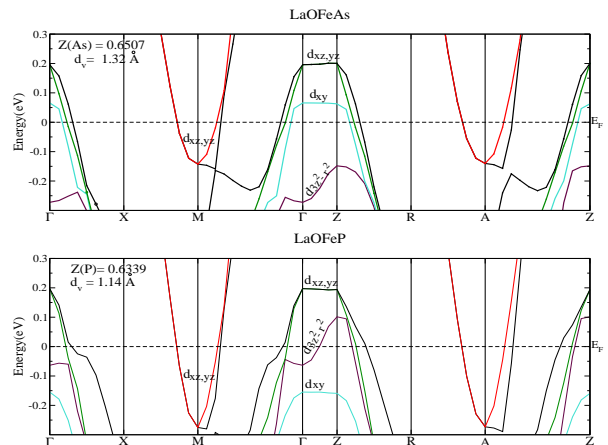


Figure 2: Low energy region of LaOFePn' s band structures with  $Pn=$  As (up panel) and P (lower panel).

neighbour Fe sites. With this choice, the  $d_{xy}$  orbital is the one that points to the  $Pn$  atom while  $d_{x^2-y^2}$  points towards the nearest-neighbor Fe.) The significant difference between these compounds comes from the third pocket centered along the  $\Gamma \rightarrow Z$  direction. In LaOFeAs this third pocket has mainly  $d_{xy}$  character and presents almost no dispersion along the  $z$ -direction (it is therefore two-dimensional (2D) in nature). In contrast, in LaOFeP it consists of a dispersing 3D pocket with mainly  $d_{3z^2-r^2}$  character.

This difference in the Fermi surfaces may explain the fact that LaOFeAs is magnetically ordered with better nesting properties than LaOFeP, for which no magnetic ordering has been reported. When the situation with the superconductivity of undoped LaOFeP gets eventually clarified, this difference in the Fermi surfaces may actually prove to be significant also in this respect.

The explanation for this difference in the low-energy band-structure, as obtained from first-principles electronic structure methods, lies mainly in its great sensitivity to the Fe- $Pn$  distance and to the vertical distance of the  $Pn$  to the Fe plane. The reason for this sensitivity is that, close to the Fermi level, there is a sizeable hybridization between Fe and  $Pn$  states as will be shown later in details.

We checked the effect of doping by using the virtual crystal approximation. We observe that for the experimental structures there are no qualitative changes in the low energy band-structure for LaOFeAs, only a shift of the chemical potential with still three 2D-like pockets crossing the Fermi level. In contrast, for LaOFeP, the 3D pocket gets filled and almost disappears from the Fermi surface in the doped compound. One should note that the bandstructure and FS properties obtained for the *relaxed* LaOFeAs structure (in contrast to the experimental one) using LDA (also reported by Singh<sup>13</sup>) presents features that are very similar to the ones described above for the LaOFeP material. This is due to the fact that LDA overestimates the Fe-As bonding,

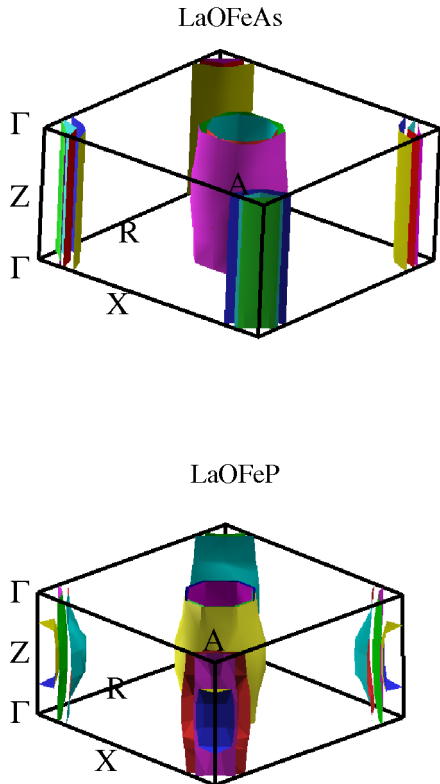


Figure 3: Fermi surfaces for LaOFeAs and LaOFeP calculated at their experimental crystal structure.

so that the Fe-As distance ( $\sim 2.4 \text{ \AA}$  experimentally) in the relaxed structure becomes as small as in the LaOFeP compound, which is around  $2.3 \text{ \AA}$ . As a result, the LDA relaxed structure of LaOFeAs displays a 3D pocket which disappears upon doping.

In order to understand better the sensitive dependence of the low-energy bandstructure on the  $Pn$  height with respect to the Fe plane, we have studied the LaOFeAs system by fixing the lattice parameters  $a$  and  $c$  at their experimental values, while varying the vertical position of As all the way from the experimental value down to a position which is very close to the one that P has in the LaOFeP material (see Table I).

The results of this study are depicted on Fig.4. We see from this figure that the 2D pocket with  $d_{xy}$  character in the ‘experimental’ LaOFeAs (upper panel) evolves into a 3D pocket with  $d_{3z^2-r^2}$  character as As is moved closer to the plane (lowest panel). The circles in the plots indicate As contribution (mainly As- $p_z$ ) to the  $d_{3z^2-r^2}$ .

In a nutshell, one can say that ‘LaOFeAs evolves into LaOFeP’ as the height of the As to the Fe plane de-

creases.

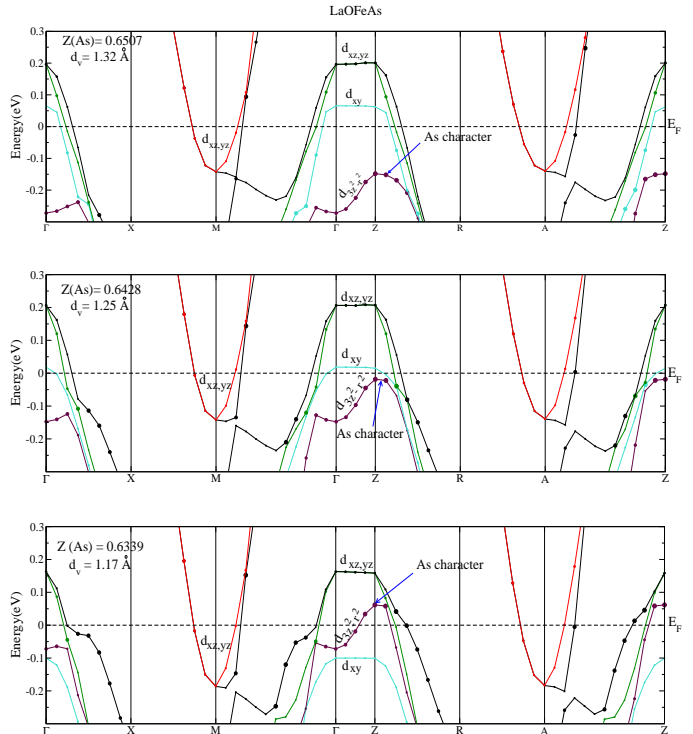


Figure 4: Sensitivity of the low energy band structure for LaOFeAs to  $d_v$  (As’ s vertical distance with respect to the Fe plane) for fixed lattice constants  $a$  and  $c$ . The considered  $d_v$  values are indicated in each plot.

#### IV. ANALYSIS IN TERMS OF WANNIER FUNCTIONS

In the previous section we have noted that the low-energy band structure, and most notably the topology of the Fermi surface depend very sensitively on the internal structural parameter  $z(\text{As})$ . Reducing  $z(\text{As})$  amounts to decreasing the distance of the As ions to the Fe plane, and changing accordingly the angle that the Fe-As bond is forming with the Fe-plane. In this section, we obtain more direct insights into this sensitive dependence by constructing Wannier functions, which reveal the strong covalency and hybridization effects associated with the Fe-As bond. We present calculations done at the experimental structural parameters.

We have used two different types of Wannier constructions. The first one is a maximally localized Wannier function construction (MLWF)<sup>21</sup> based on an ultra-soft pseudopotential approach as implemented in the PWSCF code<sup>19</sup>. The second one is the N-th Order Muffin Tin Orbitals (NMO) method and downfolding technique<sup>23</sup>, based on an LMTO-ASA approach<sup>24</sup>. Previous experience has shown<sup>25</sup> that these two approaches give results that are quite comparable to each other.

Spread (in Å)	d-downfolding	dpp-downfolding
$z^2$	1.78	1.02
xz	2.05	1.25
yz	2.05	1.25
xy	2.36	1.24
$x^2 - y^2$	1.73	0.97
As-p		1.87
As-p		1.92
As-p		1.92
O-p		1.26
O-p		1.28
O-p		1.28

Table II: Spread of maximally localized Wannier functions, both for a model retaining only the Fe-d states and a model that also includes As- and O-p orbitals. Note in particular the large spread of the  $xy$  orbital, which points towards the As atom.

A crucial issue is the choice of the energy range on which the downfolding is performed, i.e the set of Bloch bands that the Wannier construction aims at reproducing. We shall consider two possible choices: a restricted energy range covering roughly  $[-2, +2]$ eV around the Fermi level, corresponding to downfolding on the set of  $2 * 5$  bands with dominant Fe character. We shall call this the ‘d-downfolding’. We have also consider downfolding on a much larger energy range (approximately from  $-6$ eV to  $+2$ eV) encompassing all bands with Fe-d, O-p and As-p character ( $2 * 11$  bands), which we shall denote by ‘dpp-downfolding’.

In Table II, we display our results for the spatial extension of the various Wannier functions of LaOFeAs obtained by the MLWF construction, for both choices of downfolding, as measured by the spread:  $\Omega = \sqrt{\langle r^2 \rangle - \langle r \rangle^2}$ . The most striking feature is the large values of the spreads, in particular of the  $d_{xy}$  orbital which points towards the As-atoms, when downfolding is performed on the restricted set of Fe bands. Note that the spread of the  $d_{xy}$  orbital is actually comparable to the Fe-As distance. The spreads are considerably reduced when performing the *dpp*-downfolding involving the larger set of bands, as expected.

In order to visualize this effect, we plot in Fig. 5(a) the isosurface of the  $xy$ -like Wannier function. The ‘leakage’ of the Fe state on the neighboring As atoms is clearly visible. In Fig. 5(b) we plot the same isosurface for the same  $d_{xy}$  orbital, but in the ‘*dpp*’ Wannier construction. As expected, the orbitals are considerably more localised in this case, and the leakage onto the neighboring As atoms is suppressed.

In passing, we note that these observations have direct implications for many-body calculations of these materials performed within the dynamical mean-field theory

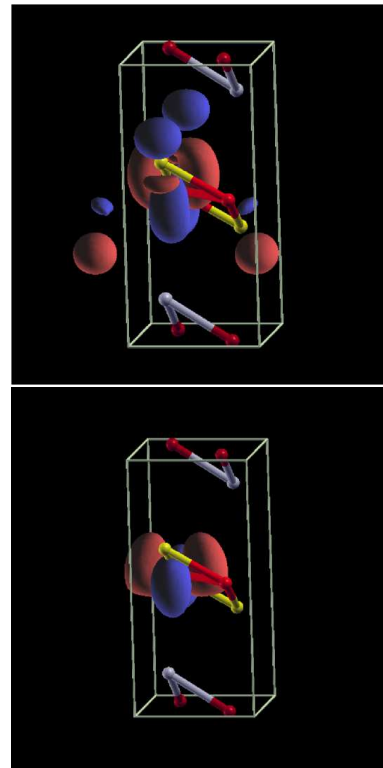


Figure 5: (a) Fe- $xy$  Wannier function for LaFeOAs, from the maximally localized Wannier construction performed for the restricted set of Fe-like bands (d-downfolding). (b) Same orbital character, but within the dpp downfolding, retaining the full set of Fe-d As-p and O-p bands.

(DMFT) framework. Because of the spatially extended character of the Fe-Wannier functions in the restricted d-downfolding, it seems that including only local matrix elements of the Coulomb interaction and local components of the self-energy would be a rather poor approximation for this ‘d-only’ model. A full model using dpp-downfolding (hence with more local Wannier functions) seems like a better starting point for a DMFT calculation. This observation may help understanding some of the differences recently reported in DMFT calculations of LaOFeAs<sup>2,26</sup>. However, another important issue is the value of the on-site Coulomb interaction and the efficiency of screening, which determines whether these materials should be viewed as in the intermediate or strong correlation regime.

Finally, in Fig. 6, we display cuts through the isosurfaces of some of the Wannier functions obtained within the NMTO construction within d-downfolding. More specifically, we have chosen to visualise the most extended orbital ( $xy$ ), the least extended one ( $x^2 - y^2$ ), and the  $3z^2 - r^2$  which due to its orientation along the  $z$ -axis plays a special role. Also, as shown in the previous section, the roles of the  $xy$  and the  $3z^2 - r^2$  orbitals somewhat interchange concerning the Fermi surface properties when the  $z$  parameter is varied.

We display three specific cuts: the first two are parallel

to the Fe  $xy$ -plane and correspond to (i) the Fe-plane, (ii) a plane containing the lower layer of pnictide atoms. The last one is (iii) a cut along a plane parallel to the  $z$ -axis and containing a nearest-neighbour Fe-As bond. It thus cuts through half of the La, Fe, O and As atoms in the unit cell. While the first cut mainly gives the orientation of the Fe orbital, the other two are measures of the leakage of the iron orbitals onto the As states. The cuts are represented in the three columns of Fig. 6, the rows show three different Fe-d orbitals:  $xy$ ,  $3z^2 - r^2$  and  $x^2 - y^2$ .

The first panel in Fig. 6 shows the  $xy$ -orbital – the one pointing towards the As atoms – of the Fe atom at the center of the plot. Also clearly visible are the contributions of this orbital on the neighboring four Fe atoms, as well as parts of the lobes of the four next nearest neighbor Fe atoms. Note, that the two As atoms do not lie in the plane represented here, but 1.32 Å above and below respectively. Still, they mediate the hopping to the next nearest Fe atoms, which display more extended  $xy$ -character than the nearest neighbours, consistent with the observation of strong nearest neighbor hopping. The second plot in the first row of Fig. 6 shows this same Fe orbital but represented by an isosurface cut containing the As-plane. The contributions of the Fe orbital leaking into this plane and in particular onto the two As atoms (eye-like features) are clearly visible. Finally, the cut of this orbital in the plane containing the  $z$ -axis confirms the very extended nature of this orbital.

The second row in Fig. 6 shows the same cuts, but for the  $3z^2 - r^2$  orbital, the third row for the  $x^2 - y^2$  orbital. Particularly interesting are the second plots in these rows which visualise the hybridisation with the  $p_x \pm ip_y$  orbitals of the As atoms, respectively. For LaFeOP (not shown) a similar picture emerges.

The overall comparison of the different orbitals confirms the result of Table 1 that the  $xy$  orbital is by far the most extended one (followed in fact by the  $yz$  and  $xz$  orbitals – not shown), displaying a tremendous contribution on the neighboring As sites, in a pancake-like flat shape. Fig. 7 shows the partial densities of states (DOS) of the different Fe-d orbitals, in comparison with the As partial DOS. The pronounced peaks of the  $xy$  and the  $xz/yz$  densities of states in the region of the As-p bands demonstrate once more that the large spatial extension of these orbitals is due to their hybridising with the As-p states.

The Wannier analysis can thus be summarized saying that it shows the large extension of the d-orbitals when a d-downfolding is used, with the  $xy$ - [ $3z^2 - r^2$ ] being the most [least] extended one. This leakage is consistent with the high sensitivity of the low energy electronic structure with respect to the  $z$  parameter observed in the previous section.

## V. WIDTH OF THE IRON BANDS: MATERIALS DEPENDENCE

Having documented in the previous sections (especially from a comparison of LaOFeP and LaOFeAs) the importance of covalency and of the Fe- $Pn$  distance, we finally turn to the influence of structural properties on the bandwidth of the iron bands, in a broader context. This question has very recently attracted attention, with the observation by Zhao *et al.*<sup>27</sup> of an apparent systematic correlation between the superconducting critical temperature of several different As-based pnictides and the angle formed by the Fe-As bond with respect to the Fe-basal plane. Specifically, these authors observed that the various materials under consideration have comparable Fe-As distance (bond-length)  $d_{Fe-As}$  while the in-plane lattice parameter  $a$  decreases as  $T_c$  increases. Furthermore, these authors suggested that this may imply a smaller bandwidth  $W$  for materials with highest  $T_c$ , and hence that superconductivity is enhanced by increasing correlation strength (increasing  $U/W$  ratio). Note, however, that this would mean a smaller bandwidth with decreasing Fe-Fe distance.

Denoting by  $\theta$  the angle formed by the Fe-As bond with respect to the basal plane as sketched in Fig. 8 (so that the opening angle at the top of the  $Fe_4As$  pyramid is  $\theta_3 = \pi - 2\theta$  in the notations of Ref. 27), the interatomic distances characterizing the Fe-As unit and the vertical distance of As with respect to the basal Fe plane are given by:

$$d_{Fe-Fe} = \frac{a}{\sqrt{2}}, \quad d_{Fe-As} = \frac{a}{2 \cos \theta}, \quad (1)$$

$$d_v = \frac{a}{2} \tan \theta = c \left( z(As) - \frac{1}{2} \right)$$

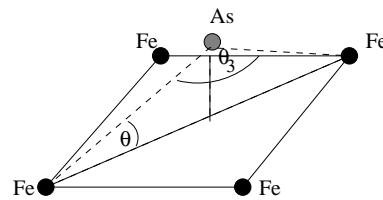


Figure 8: Schematic  $Fe_4As$  pyramid for LaOFeAs. The  $\theta$  and  $\theta_3$  angles are indicated.

In order to investigate the dependence of the bandwidth on these structural parameters, we performed the following studies, which can be viewed as ‘numerical experiments’:

- (i) Keeping the lattice constants  $a$  and  $c$  at their experimental values in undoped LaOFeAs, we studied how the band-structure evolves as the As is brought into the plane, starting from its experimental position down to a value comparable to the

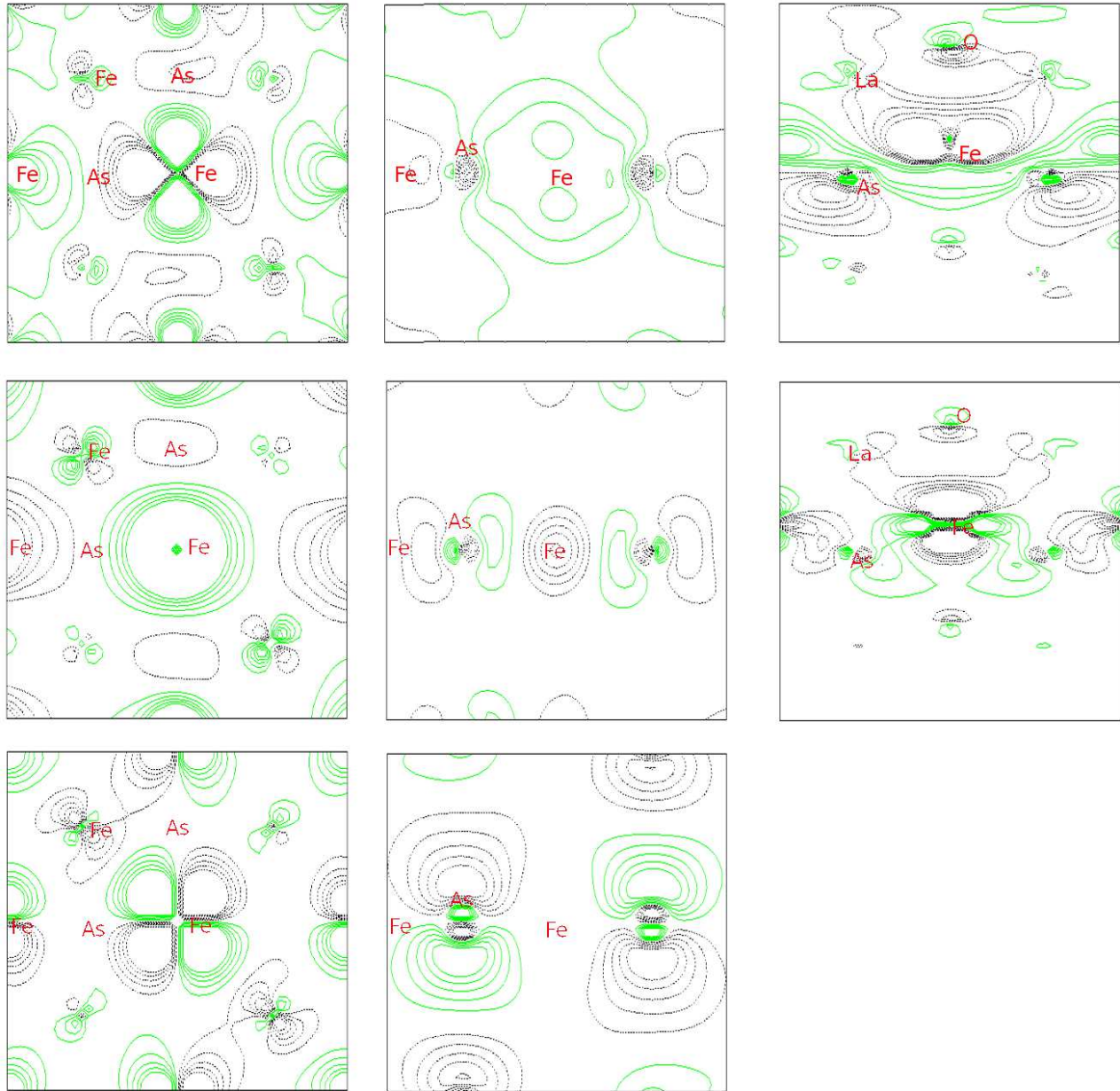


Figure 6: Fe orbitals for the 5-band model for LaFeOAs. First row:  $xy$  orbital. Second row:  $3z^2 - r^2$  orbital. Third row:  $x^2 - y^2$  orbital. In the Fe-plane (first column), in the lower As-plane (second column) and in a plane parallel to the  $z$ -axis containing one La, O, Fe, As per unit cell (third column). In the first two columns the  $x$ -axis is along the diagonal of the plots. Note that the  $x^2 - y^2$  orbital has nodes in the latter plane and is thus not shown in this representation.

height of P in the LaOFeP compound, i.e reducing  $d_v$  or  $z(\text{As})$  (hence decreasing  $\theta$  and increasing  $\theta_3$ ). The resulting changes in the low-energy electronic structure corresponding to these calculations have been reported above in Sec. III

- (ii) Keeping constant the Fe-As distance  $d_{\text{Fe-As}} = 2.407 \text{ \AA}$  (as well as  $c$  at the same value than above),

we reduce the lattice parameter  $a$ . In so doing, the vertical distance  $d_v$  separating As from the Fe plane increases, resulting in a larger angle  $\theta$  with the basal plane and a smaller angle at the summit  $\theta_3$ .

- (iii) Finally, we consider the actual experimental structure of the parent compounds LaOFeAs, PrO-

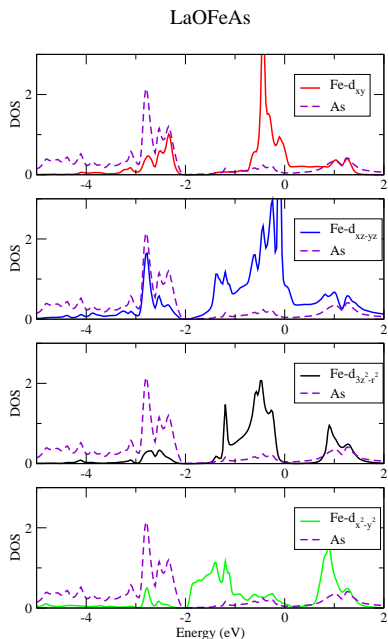


Figure 7: Partial density of states of the Fe-d orbitals (solid lines), compared to the As density of states (dashed lines, same curve in all panels).

FeAs and SmOFeAs. These three materials have almost identical Fe-As distance and correspond to decreasing values of  $a$ , similarly to (ii), but in contrast to this case they also correspond to decreasing values of the lattice constant  $c$ , with the ReO unit getting closer to the FeAs one.

The results of these investigations are depicted in Fig. 9, in which we display the change in both the full bandwidth  $W$  of the Fe bands and the bandwidth of the occupied Fe states  $W_{occ}$  (i.e the distance from the bottom of the Fe bands up to Fermi level). Both quantities provide useful information, but the latter is usually a better assessment of the relative importance of correlation effects (being related to the typical kinetic energy).

We note the following trends for the three numerical experiments above:

- (i) As  $d_v$  is reduced for fixed  $a$ , a systematic increase of the bandwidth (and of the bandwidth of the occupied states) is observed. This is indeed expected: the direct Fe-Fe hopping is unchanged, while hybridisation effects with As are increased as  $d_v$  is decreased, hence increasing the hopping through As sites. Thus, in this case, the bandwidth *decreases* as  $\theta_3$  decreases (and  $\theta$  increases).
- (ii) In this case where  $d_{Fe-As}$  is kept constant, both the occupied and full bandwidth show a smaller effect as the  $a$  parameter decreases. Hence, there is a slight dependence of the bandwidth on the angles  $\theta, \theta_3$  as compared to i). The reason for this is that the increased Fe-Fe hopping (due the decrease of  $a$ )

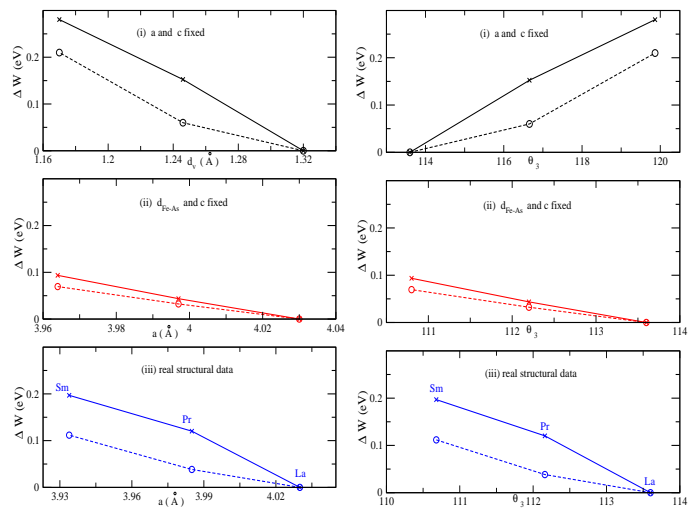


Figure 9: The change  $\Delta W$  in the Fe 3d full bandwidth  $W$  (solid line) and the bandwidth of its occupied part  $W_{occ}$  (dashed line) with respect to calculated value for LaOFeAs at its experimental structure<sup>5</sup>. These reference values are 4.25 eV for  $W$  and 1.95 eV for  $W_{occ}$ . From the top to bottom panels we display the results for the calculations i), ii), iii) as explained in the text. Left:  $\Delta W$  as a function of  $d_v$  or  $a$ , as indicated. Right:  $\Delta W$  as a function of  $\theta_3$ . The structural data for Pr and Sm compounds were taken from Ref. 28 and 29, respectively.

is precisely compensated by the decrease of indirect hopping through As (due to the increase of  $d_v$ ).

- (iii) Finally, for the real materials which also have basically a constant  $d_{Fe-As}$ , we observe nevertheless a stronger *increase* of the bandwidth as  $a$  is reduced as compared to ii). The reason for the difference with (ii) is that the lattice parameter  $c$  simultaneously decreases, and indeed the increase of the bandwidth comes also from unoccupied bands above Fermi-level, reflecting the influence of the Re-O unit becoming closer. Hence, for the three materials investigated, the bandwidth *increases* as  $\theta_3$  decreases (and  $\theta$  increases), in contrast to (i). The *occupied* bandwidth is even less sensitive to  $\theta_3$ , again because of the compensating effect observed for (ii).

The general conclusion of this investigation is that, as expected physically, the bandwidth is controlled both by the direct Fe-Fe hopping in the plane and by the indirect hopping through As (in view of covalency and hybridization effects). Both the parameters  $a$  and  $\theta$  (or  $\theta_3$ ) are therefore important. The bandwidth can in principle behave differently (increase or decrease) as the opening angle  $\theta_3$  is decreased. For the three real materials that we have investigated, the bandwidth displays a sizable *increase* for decreasing  $\theta_3$  however, in contradiction to the proposal made in Ref. 27. This increase is basically related to the decrease of the  $c$ -parameter and the increase

Fe-Fe hopping (at constant  $c$  the bandwidth experiments a more slight effect).

## VI. CONCLUSIONS

The iron oxypnictides family of compounds share a similar overall electronic structure. Some important aspects, however, depend very sensitively on small structural changes, particularly on changes of interatomic distances and bond angles within the iron-pnictide plane. Using first-principles full-potential electronic structure calculations, we investigate this sensitive dependence, contrasting in particular LaOFeAs and LaOFeP, which display different transport, magnetic and superconducting properties. The width of the Fe-bands is significantly larger for LaOFeP, indicating a better metal and weaker electronic correlations. These two materials also present significant differences in their very low-energy bandstructure, when calculations are performed at their experimental crystal structure. Both materials have three hole-pockets around the  $\Gamma$  point and two electron pockets around the M-point. However, one of the hole pockets changes from a three-dimensional one to a tube with two-dimensional dispersion when going from LaOFeP to LaOFeAs. These differences are due to the shorter Fe-Fe distance and to the shorter distance of the pnictide to the iron-plane in LaOFeP. We have shown

that the low-energy bandstructure of LaOFeAs evolves towards that of LaOFeP as the As atom is lowered from its experimental position to a position closer to the Fe plane. We argue that the physical origin of this sensitivity to the iron-pnictide distance is the covalency of the iron-pnictide bond, leading to strong hybridization effects. To illustrate this, we have constructed Wannier functions which are found to have a large spatial extension when restricting the energy window to the bands with dominant iron character. Finally, we have clarified how the bandwidth changes as one moves along the rare-earth series in ReOFeAs. Since the Fe-As distance remains essentially constant, the Fe-Fe distance contracts while the vertical distance to the Fe plane increases, resulting in a compensating effect and rather small changes of the bandwidth. A slight increase of the bandwidth of unoccupied states is observed, which is actually associated with the decreasing distance between the Fe-As and Re-O planes.

## Acknowledgments

This work has been supported by the French ANR under project ETSF, and a computing grant at IDRIS Orsay (project 081393). We acknowledge useful discussions with J. Bobroff and K. Nakamura.

- 
- <sup>1</sup> Y. Kamihara, T. Watanabe, M. Hirano, and H. Hosono, *J. Am. Chem. Soc.* **130**, 3296 (2008).
- <sup>2</sup> K. Haule, J.H. Shim, and G. Kotliar, arXiv:0803.1279v1 (2008).
- <sup>3</sup> I.I. Mazin, D.J. Singh, M.D. Johannes, and M.H. Du, arXiv:0803.2740 (2008).
- <sup>4</sup> V. Cvetkovic and Z. Tesanovic, arXiv:0804.4678 (2008).
- <sup>5</sup> C. de la Cruz, Q. Huang, J.W. Lynn, J. Li, W. Ratcliff II, J.L. Zarestky, H.A. Mook, G.F. Chen, J.L. Luo, N.L. Wang, and P. Dai, *Nature* **453**, 899 (2008).
- <sup>6</sup> D. Johnson and W. Jeitschko, *J. Solid State Chem.* **11**, 161 (1974).
- <sup>7</sup> Y. Kamihara, H. Hiramatsu, M. Hirano, R. Kawamura, H. Yanagi, T. Kamiya, and H. Hosono, *J. Am. Chem. Soc.* **128**, 10012 (2006).
- <sup>8</sup> J.P. Carlo, Y.J. Uemura, T. Goko, G.J. MacDougall, J.A. Rodriguez, W. Yu, G.M. Luke, Pengcheng Dai, N. Shannon, S. Miyasaka, S. Suzuki, S. Tajima, G.F. Chen, W.Z. Hu, J.L. Luo, and N.L. Wang, arXiv:0803.2703 (2008).
- <sup>9</sup> Y. Kamihara, M. Hirano, H. Yanagi, T. Kamiya, Y. Saitoh, E. Ikenaga, K. Kobayashi, and H. Hosono, arXiv:0805.2983 (2008).
- <sup>10</sup> T. M. McQueen, M. Regulacio, A. J. Williams, Q. Huang, J. W. Lynn, Y. S. Hor, D.V. West, M. A. Green, R. J. Cava, arXiv:0805.2149 (2008).
- <sup>11</sup> S. Lebegue, *Phys. Rev. B* **75**, 035110 (2007).
- <sup>12</sup> L. Boeri, O.V. Dolgov, and A.A. Golubov, arXiv:0803.2703 (2008).
- <sup>13</sup> D.J. Singh and M.H. Du, arXiv:0803.0429 (2008).
- <sup>14</sup> I.I. Mazin, M.D. Johannes, L. Boeri, K. Koepernik, and D. J. Singh, arXiv:0806.1869 (2008).
- <sup>15</sup> Z. P. Yin, S. Lebegue, M. J. Han, B. Neal, S. Y. Savrasov, W. E. Pickett, arXiv:0804.3355 (2008).
- <sup>16</sup> P. Blaha, K. Schwarz, G.K.H. Madsen, D. Kvasnicka, and J. Luitz, WIEN2K, An augmented planewave+local orbitals program for calculating crystal properties (Technische Universitat Wien, 2002, Austria); <http://www.wien2k.at>
- <sup>17</sup> Perdew J.P. and Wang Y. 1992, *Phys.Rev.* B45, 13244
- <sup>18</sup> Perdew J.P., Burke S. and Ernzerhof M. 1996, *Phys.Rev.Let.* 77, 3865
- <sup>19</sup> S. Baroni, A. Dal Corso, S. de Gironcoli, P. Giannozzi, C. Cavazzoni, G. Ballabio, S. Scandolo, G. Chiarotti, P. Focher, A. Pasquarello, K. Laasonen, A. Trave, R. Car, N. Marzari, and A. Kokalj, <http://www.quantum-espresso.org>
- <sup>20</sup> K. Kuroki, S. Onari, R. Arita, H. Usui, Y. Tanaka, H. Kontani, and H. Aoki, arXiv:0803.3325 (2008).
- <sup>21</sup> N. Marzari, D. Vanderbilt, *Phys. Rev. B* **56**, 12847 (1997).
- <sup>22</sup> <http://www.wannier.org>.
- <sup>23</sup> O. K. Andersen and T. Saha-Dasgupta, *Phys. Rev. B* **62**, R16219 (2000).
- <sup>24</sup> O. K. Andersen and O. Jepsen, *Phys. Rev. Lett.* **53**, 2571 (1984).
- <sup>25</sup> F. Lechermann, A. Georges, A. Poteryaev, S. Biermann, M. Posternak, A. Yamasaki, and O. K. Andersen, *Phys. Rev. B* **74**, 125120 (2006).
- <sup>26</sup> A.O. Shorikov, M.A. Korotin, S.V. Streltsov, S.L. Sko-

- rnyakov, D.M. Korotin, V.I. Anisimov, arXiv:0804.3283.
- <sup>27</sup> Zhao J., Q. Huang, C. de la Cruz, Sh. Li, J.W. Lynn, Y. Chen, M. A. Green, G.F. Chen, G. Li, Z. Li, J.L. Luo, N.L. Wang, P. Dai, arXiv: 0806.2528(2008).
- <sup>28</sup> P. Quebe, L. J. Terböchte, and W. Jeitschko, J. Alloys and Compounds **302**, 70 (2000).
- <sup>29</sup> N. D. Zhigadlo, S. Katrych, Z. Bukowski, and J. Karpinski, arXiv: 0806.0337 (2008).

